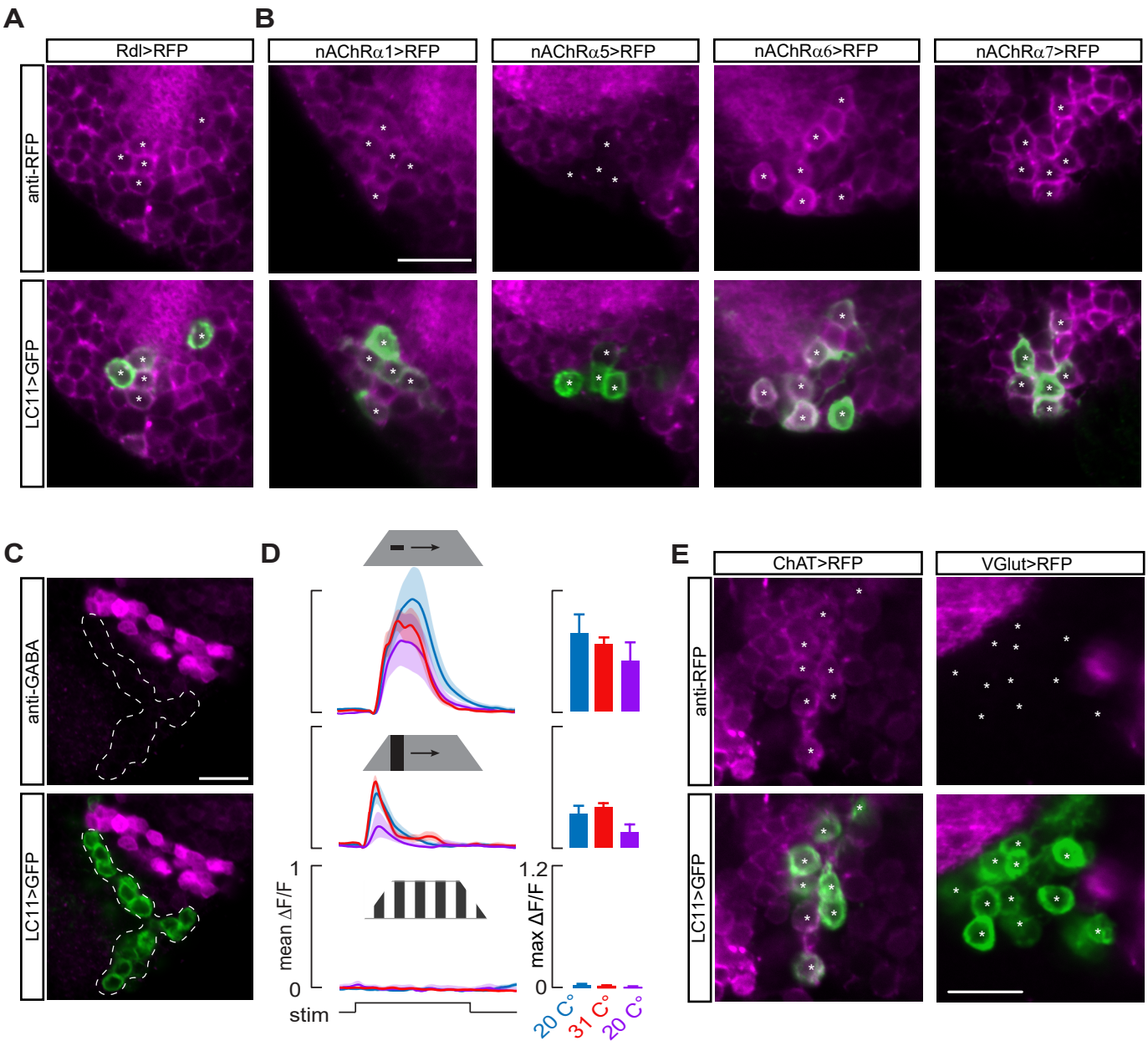
A
B
Rdl>RFP
nAChRα1>RFP
nAChRα5>RFP
nAChRα6>RFP
nAChRα7>RFP
anti-RFP
LC11>GFP
C
D
E
anti-GABA
LC11>GFP
mean ΔF/F
1
0
stim
max ΔF/F
1.2
0
20 C°
31 C°
20 C°
ChAT>RFP
VGlut>RFP
anti-RFP
LC11>GFP

Figure S1

Fig S1. LC11 express GABA-A receptor subunit *Rdl*, specific acetylcholine receptors, choline acetyltransferase (ChAT) but not vesicular glutamate transporter (VGlut) or GABA. Related to Figure 1.

(A) Confocal image of RFP (magenta) driven by $Rdl^{MI02957}$-Gal4 shown either alone (upper panel) or with GFP (green) expression driven by LC11-LexA (lower panel). (B) Confocal images of RFP (magenta) driven by $nAChRalpha1^{MI00453}$-Gal4, $nAChRalpha5^{MI13859}$-Gal4, $nAChRalpha6^{MI01466}$-Gal4 and $nAChRalpha7^{MI12545}$-Gal4 from left to right. Bottom panels are same as upper panels but with GFP driven by LC11-LexA.

(C) Confocal image of an adult brain stained with anti-GABA (magenta) and anti-GFP (green). LC11-Gal4 drives the expression of GFP. Dashed line encapsulates LC11 cell bodies.

(D) Shi^{ts} is co-expressed with GCaMP6m in LC11. The temperature of the microscope stage perfusion was controlled externally and preparations were tested at 20˚C then 31˚C then again at 20˚C. Visual stimuli were moved counterclockwise before and after temperature induced synaptic inactivation. None of the peak amplitude GCaMP6f responses are significantly different from one another. n=5. Error bars and shading indicate S.E.M.

(E) $ChAT^{MI04508}$-Gal4 and $VGlut^{MI04979}$-Gal4 drive the expression of RFP (magenta) and LC11-LexA drives the expression of GFP (green). Asterisks in panels indicates the location of cell bodies. Scale bars are 10 μm. Scale bar in B applies to both A and E.

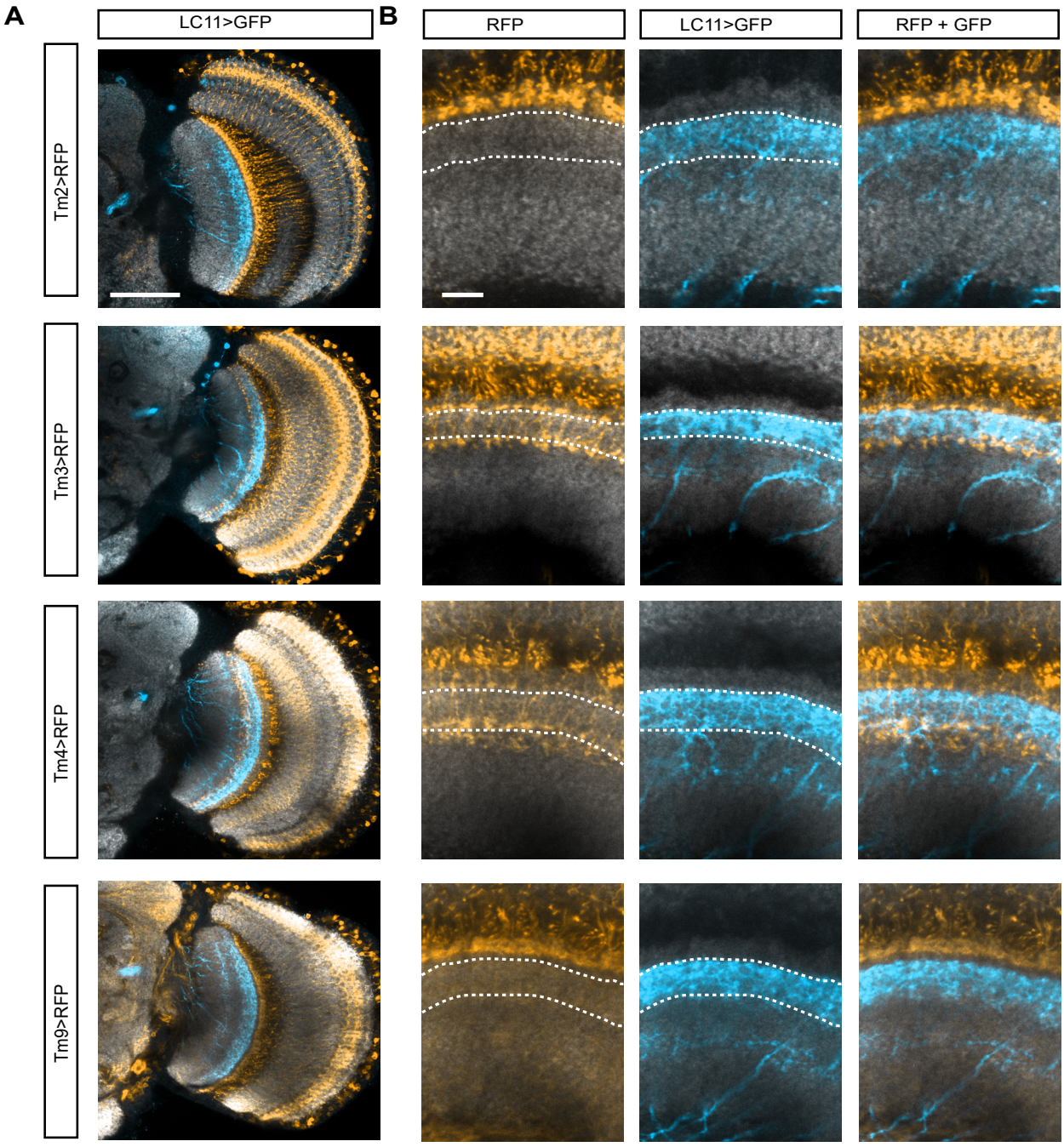

Figure S2

Fig S2. Columnar neurons innervating T5 do not overlap with LC11 dendrites, T2 and T3 neurons synapse with LC11. Related to Fig 3 A-B.
(A) LC11-LexA driving GFP (blue) and Tm2, Tm3, Tm4, Tm9 Gal4s driving RFP (yellow), anterior single plane confocal image of the right optic lobe. Scale bar is 50 μm.
(B) Cross-section of the lobula showing distal layers on top, proximal layers on bottom. LC11 dendrites are highlighted with dashed white lines. None of the terminal strata from the four medulla columnar neurons show extensive overlap with LC11 dendrites. Scale bar is 10 μm.

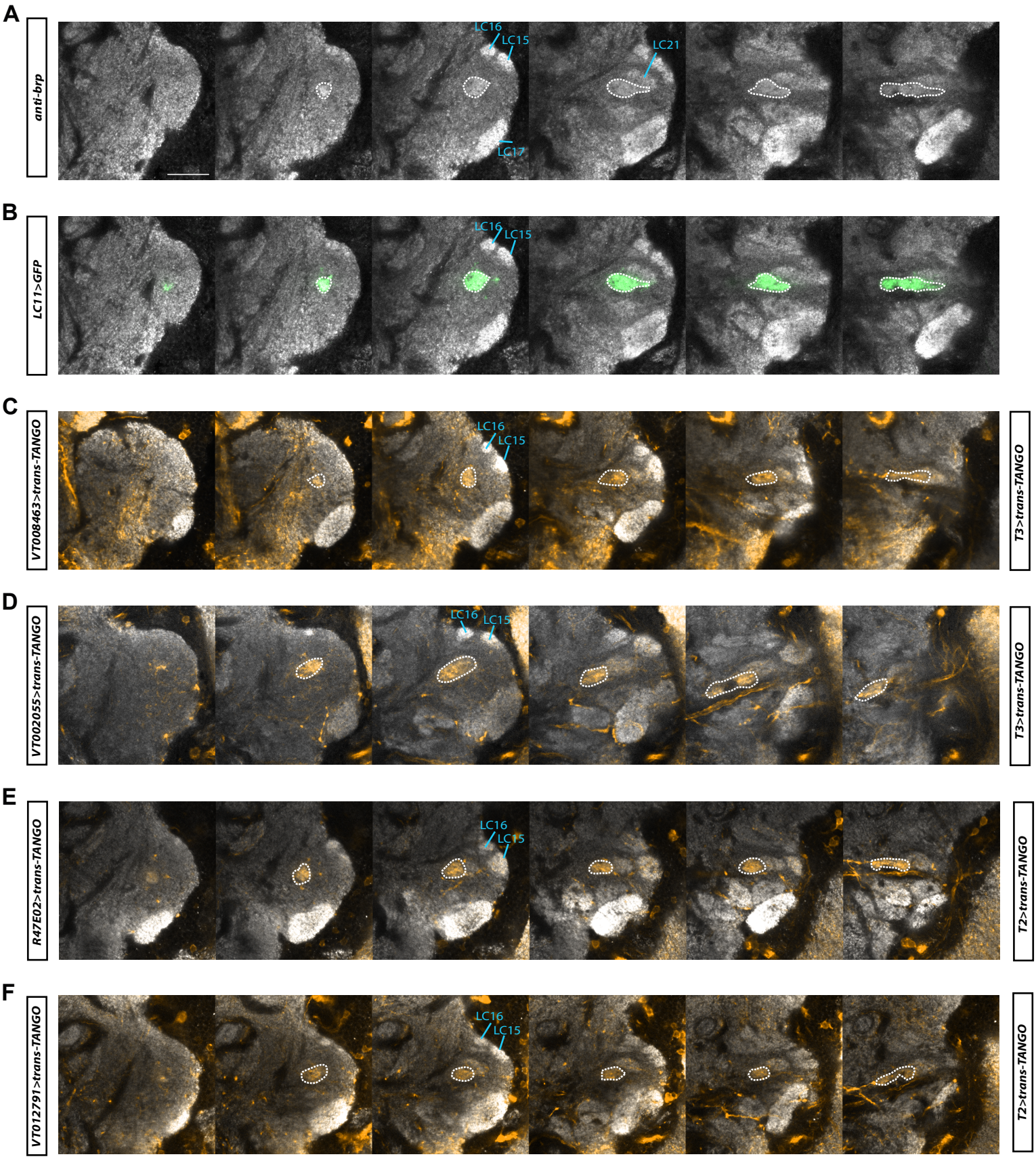
A
anti-brp
LC16
LC15
LC21
LC17
B
LC11>GFP
LC16
LC15
C
VT008463>trans-TANGO
LC16
LC15
T3>trans-TANGO
D
VT002055>trans-TANGO
LC16
LC15
T3>trans-TANGO
E
R47E02>trans-TANGO
LC16
LC15
T2>trans-TANGO
F
VT012791>trans-TANGO
LC16
LC15
T2>trans-TANGO

Figure S3

Fig S3. Anterograde synaptic labeling reagent trans-Tango expressed by either T2 or T3 label LC11 glomerulus in protocerebrum. Related to Figure 3 D-F.
(A) Confocal images of ventrolateral protocerebrum labeled with anti-Brp (gray) seen here from the anterior view. Dense brp labeling reveals previously identified optic glomeruli (blue). LC11 glomerulus is encircled with a dashed line. Scale bar is 25 μm.
(B) Same as A but with LC11-Gal4 driving the expression of GFP (green).
(C-F) Trans-Tango driven by either T2 (E and F) or T3 (C and D) labels the LC11 glomerulus in the protocerebrum. LC11 glomerulus is determined by stereotypical location relative to the other glomeruli and dense synaptic labeling. Yellow shows all cells that are post synaptic to the cells that are labeled by indicated drivers.

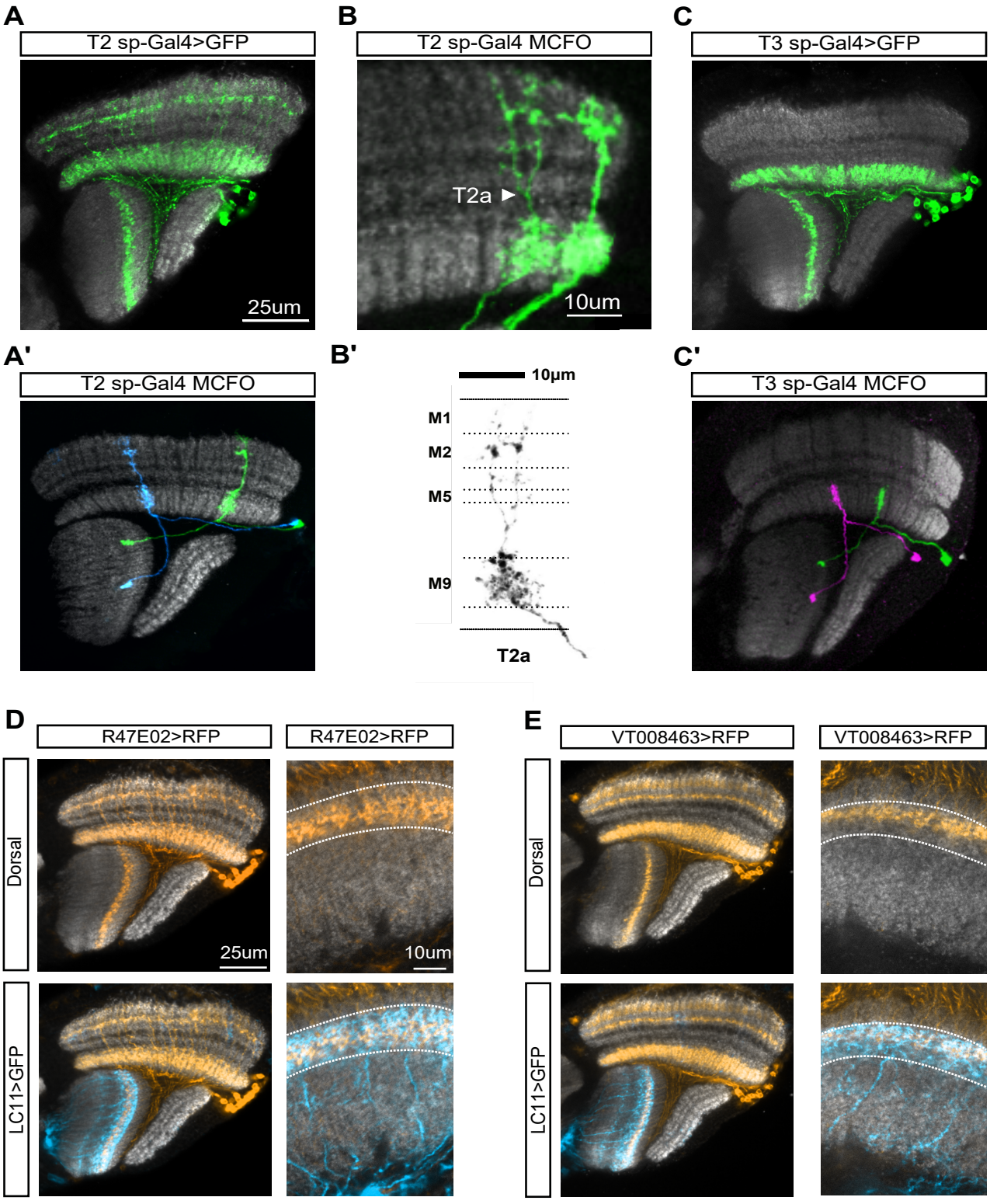
A
T2 sp-Gal4>GFP
25um
B
T2 sp-Gal4 MCFO
T2a
10um
C
T3 sp-Gal4>GFP
A'
T2 sp-Gal4 MCFO
B'
10μm
M1
M2
M5
M9
T2a
C'
T3 sp-Gal4 MCFO
D
R47E02>RFP
R47E02>RFP
Dorsal
25um
10um
LC11>GFP
E
VT008463>RFP
VT008463>RFP
Dorsal
LC11>GFP

Figure S4

Fig S4. Characterization of T2 and T3 split-Gal4s. Related to Figure 4.
(A) Confocal image of T2 sp-Gal4 driven GFP (green) seen from dorsal view.
(A') Individual T2 cells (blue and green) labeled by Multi-Color Flip Out (MCFO, (Nern et al., 2015)).
(B) Occasionally, the T2 split-Gal4 labeled possible T2a neurons defined by the prominent split neurite in the distal medulla and a less dense dendritic field.
(B') Morphology of individual candidate T2a neuron, labeled by MCFO, showing approximate innervation of layers in the medulla (top) and in the lobula (bottom).
(C) Confocal images of T3 sp-Gal4 driven GFP (green) seen from dorsal view. Scale bar is in A.
(C') Individual T3 cells (green and magenta) labeled by MCFO
(D and E). Additional drivers that are used to construct split-Gal4s. Dorsal view of the optic lobe of an adult brain expressing RFP (yellow) in T2 cells (D) and in T3 cells (E). GFP is driven by LC11-LexA in lower panels.

Fig 1B-I: w-/+;;R22H02-Gal4 (attp2), UAS-GCaMP6m (VK0005)/+

Fig 2A-G: Experimental: w-;R20G06-LexA (attP40), LexAop2-GCaMP6f (su(Hw)attp5)/ LexAop2-FLPL (attP40), LexAop2-GCaMP6f (su(Hw)attp5); Mi{Trojan-Gal4.1}Rdl[MI02957-TG4.1]/ Mi{FlpStop}Rdl[MI02620-FlpStop.ND]

Control: w-;R20G06-LexA (attP40), LexAop2-GCaMP6f (su(Hw)attP5)/ LexAop2-GCaMP6f (su(Hw)attP5); Mi{Trojan-Gal4.1}Rdl[MI02957-TG4.1]/ Mi{FlpStop}Rdl[MI02620-FlpStop.ND]

Fig 3A: 10xUAS-IVS-mCD8::RFP(attP18),13LexAop2-IVS-mCD8::GFP(su(Hw)attP8/ w-; R20G06-LexA (attP40)/+;VT012791-Gal4 (attP2)/+

Fig 3B: 10xUAS-IVS-mCD8::RFP(attP18),13LexAop2-IVS-mCD8::GFP(su(Hw)attP8/ w-; R20G06-LexA (attp40)/+;VT002055-Gal4 (attP2)/+

Fig 3C: UAS-myrGFP,QUAS-mtdTomato(3XHA)/ w-;trans-Tango/R22H02-AD (attP40);R20G06-DBD(attP2)/+;

Fig 3D: UAS-myrGFP,QUAS-mtdTomato(3XHA)/ w-;trans-Tango/+;VT012791-Gal4(attP2)/+;

Fig 3E: UAS-myrGFP,QUAS-mtdTomato(3XHA)/ w-;trans-Tango/+;VT002055-Gal4(attP2)/+;

Fig 3F: T2: w-/pBPhsFlp2::PEST (attP3); VT012791-AD (attP40)/+; R47E02-DBD (attP2)/ pJFRC201-10XUAS-FRT>STOP>FRT-myr::smGFP-HA (VK0005), pJFRC240-10XUASFRT>STOP>FRT-myr::smGFP-V5-THS-10XUAS-FRT>STOP>FRT-myr::smGFP-FLAG (su(Hw)attP1)

T3: w-/pBPhsFlp2::PEST (attP3); VT002055-AD (attP40)/+; R65B04-DBD (attP2)/ pJFRC201-10XUAS-FRT>STOP>FRT-myr::smGFP-HA (VK0005), pJFRC240-10XUASFRT>STOP>FRT-myr::smGFP-V5-THS-10XUAS-FRT>STOP>FRT-myr::smGFP-FLAG (su(Hw)attP1)

Fig 3G: T2: w-;20XUAS-GCaMP6f (attP40)/+; R47E02-Gal4 (attP2)/+ and T3: w-;20XUAS-GCaMP6f (attP40)/+;VT008463-Gal4(attP2)/+

Fig 4A-B: T2: w-;20XUAS-GCaMP6f (attP40)/+;R47E02-Gal4 (attP2)/+ and T3: w-;20XUAS-GCaMP6f (attP40)/+;VT008463-Gal4 (attP2)/+ , T4/T5: w-;R59E08-AD (attP40)/20XUAS-GCaMP6f (attP40); R42F06-DBD (attP2)/+.

Fig 4C: T2: 13XLexAop2-Syn21-opGCaMP6s (su(Hw)attP8), 10XUAS-Syn21-Chrimson88-tdT-3.1 (attP18)/ w-; R51F09-LexA (attP40)/ VT012791-AD (attP40); R47E02-DBD (attP2)/+

T3: 13XLexAop2-Syn21-opGCaMP6s (su(Hw)attP8), 10XUAS-Syn21-Chrimson88-tdT-3.1 (attP18)/ w-; R51F09-LexA (attP40)/ VT002055-AD (attP40); R65B04-DBD (attP2)/+

Fig 4D: T2: w-;13xLexAop2-Gcamp6f (su(Hw)attP5),R20G06-LexA(attP40)/ VT012791-AD (attP40); UAS-Shibire(ts1)(VK0005)/ R47E02-DBD (attP2)

T3: w-;13xLexAop2-Gcamp6f (su(Hw)attP5),R20G06-LexA(attP40)/ VT002055-AD(attP40); UAS-Shibire(ts1)(VK0005)/ R65B04-DBD (attP2)

Fig S1A: 10xUAS-IVS-mCD8::RFP(attP18),13LexAop2-IVS-mCD8::GFP(su(Hw)attP8/ w-; R22H02-LexA (attP40)/ +; Rdl[MI02957-TG4.1]/+

Fig S1B Left to Right: 10xUAS-IVS-mCD8::RFP(attP18),13LexAop2-IVS-mCD8::GFP(su(Hw)attP8/ w^-; R22H02-LexA (attP40)/+; nAChRalpha1[MI00453-TG4.0]/+

10xUAS-IVS-mCD8::RFP(attP18),13LexAop2-IVS-mCD8::GFP(su(Hw)attP8/ w^-; R22H02-LexA (attP40)/ nAChRalpha5[MI13859-TG4.2]; +/+

10xUAS-IVS-mCD8::RFP(attP18),13LexAop2-IVS-mCD8::GFP(su(Hw)attP8/ w^-; R20G06-LexA (attP40)/ nAChRalpha6[MI01466-TG4.1]; +/+

10xUAS-IVS-mCD8::RFP(attP18),13LexAop2-IVS-mCD8::GFP(su(Hw)attP8/nAChRalpha7[MI12545-TG4.1]; R20G06-LexA (attp40)/ +;+/+

Fig S1C: w^-; 10XUAS-IVS-mCD8::GFP (attP40)/+; R22H02-Gal4 (attP2)/+

Fig S1D: w^-/+;;R22H02-Gal4 (attp2), UAS-GCaMP6m (VK0005)/ 20XUAS-TTS-Shibire-ts1-p10

Fig S1E: 10xUAS-IVS-mCD8::RFP(attP18),13LexAop2-IVS-mCD8::GFP(su(Hw)attP8/ w^-; R22H02-LexA (attP40)/ +; ChAT[MI04508-TG4.0]/+

10xUAS-IVS-mCD8::RFP(attP18),13LexAop2-IVS-mCD8::GFP(su(Hw)attP8/ w^-; R22H02-LexA (attP40)/ VGlut[MI04979-TG4.2]; +/+

Fig S2: Tm2: 10xUAS-IVS-mCD8::RFP(attP18),13LexAop2-IVS-mCD8::GFP(su(Hw)attP8/ w^-; R22H02-LexA (attP40)/+; VT12282-Gal4(attP2)/+

Tm3: 10xUAS-IVS-mCD8::RFP(attP18),13LexAop2-IVS-mCD8::GFP(su(Hw)attP8/ w^-; R22H02-LexA (attP40)/+; R13E12-Gal4(attP2)/+

Tm4: 10xUAS-IVS-mCD8::RFP(attP18),13LexAop2-IVS-mCD8::GFP(su(Hw)attP8/ w^-; R22H02-LexA (attP40)/+; R35H01-Gal4(attP2)/+

Tm9: 10xUAS-IVS-mCD8::RFP(attP18),13LexAop2-IVS-mCD8::GFP(su(Hw)attP8/ w^-; R22H02-LexA (attP40)/+; 0137-Gal4(attP2)/+

Fig S3A and B: UAS-myrGFP,QUAS-mtdTomato(3XHA)/ w^-;trans-Tango/R22H02-AD (attP40);R20G06-DBD(attP2)/+;

Fig S3C: UAS-myrGFP,QUAS-mtdTomato(3XHA)/ w^-;trans-Tango/+; VT008463-Gal4 (attP2)/+;

Fig S3D: UAS-myrGFP,QUAS-mtdTomato(3XHA)/ w^-;trans-Tango/+; VT002055-Gal4 (attP2)/+;

Fig S3E: UAS-myrGFP,QUAS-mtdTomato(3XHA)/ w^-;trans-Tango/+; R47E02-Gal4 (attP2)/+;

Fig S3F: UAS-myrGFP,QUAS-mtdTomato(3XHA)/ w^-;trans-Tango/+; VT012791-Gal4 (attP2)/+;

Fig S4A: w^-;10xUAS-IVS-mCD8::GFP (attP40)/VT012791-AD (attp40); R47E02-DBD (attP2)/+;

Fig S4A'-B': T2: w^-/pBPhsFlp2::PEST (attP3); VT012791-AD (attP40)/+; R47E02-DBD (attP2)/ pJFRC201-10XUAS-FRT>STOP>FRT-myr::smGFP-HA (VK0005), pJFRC240-10XUASFRT>STOP>FRT-myr::smGFP-V5-THS-10XUAS-FRT>STOP>FRT-myr::smGFP-FLAG (su(Hw)attP1)

Fig S4C: w^-;10xUAS-IVS-mCD8::GFP (attP40)/VT002055-AD (attP40); R65B04-DBD (attP2)/+;

Fig S4C': w^{-}/pBPhsFlp2::PEST (attP3); VT002055-AD (attP40)/+; R65B04-DBD (attP2)/ pJFRC201-10XUAS-FRT>STOP>FRT-myr::smGFP-HA (VK0005), pJFRC240-10XUASFRT>STOP>FRT-myr::smGFP-V5-THS-10XUAS-FRT>STOP>FRT-myr::smGFP-FLAG (su(Hw)attP1)

Fig S4D: 10xUAS-IVS-mCD8::RFP(attP18),13LexAop2-IVS-mCD8::GFP(su(Hw)attP8/w^{-}; R20G06-LexA (attP40)/+;R47E02-Gal4 (attP2)/+

Fig S4E: 10xUAS-IVS-mCD8::RFP(attP18),13LexAop2-IVS-mCD8::GFP(su(Hw)attP8/w^{-}; R20G06-LexA (attP40)/+;VT008463-Gal4 (attP2)/+

Table S1. Genotypes used in each figure panel. Related to STAR Methods.